Electronic Supplementary Material (ESI) for Physical Chemistry Chemical Physics.

SUPPORTING INFORMATION

Maltose Binding Protein Effectively Stabilizes the Partially Closed Conformation of the ATP-binding Cassette Transporter $MalFGK_2$

Jingwei Weng, Shuo Gu, Xin Gao, Xuhui Huang*, Wenning Wang*

SUPPLEMENTARY FIGURES

Figure S1: Residues forming the periplasmic, middle and cytoplasmic gates along translocation pathway at the MalF-MalG interface and the correlation of the inter-residue distance with CV^{TMD}.

Figure S2: Top view of NBD dimer interface and the correlation between CV^{NBD} and the inter-residue distance $S83^{A}$-$S83^{B}$ at the interface.

Figure S3: Convergence check of the metadynamics simulations of the **apo** and **complex** systems.

Figure S4: The variation of C_α RMSDs along the eight 100-ns trajectories of the **complex**, **apo**, and **MalF500** systems.

Figure S5: Comparison of C_α RMSFs calculated by the unbiased **complex** and **apo** trajectories with those derived from the B-factors of the crystal structures.

Figure S6: Projections of snapshots from eight 100-ns **complex** and **apo** trajectories initiated from intermediate structure on the 2-D space spanned by CV^{NBD} and CV^{TMD}.

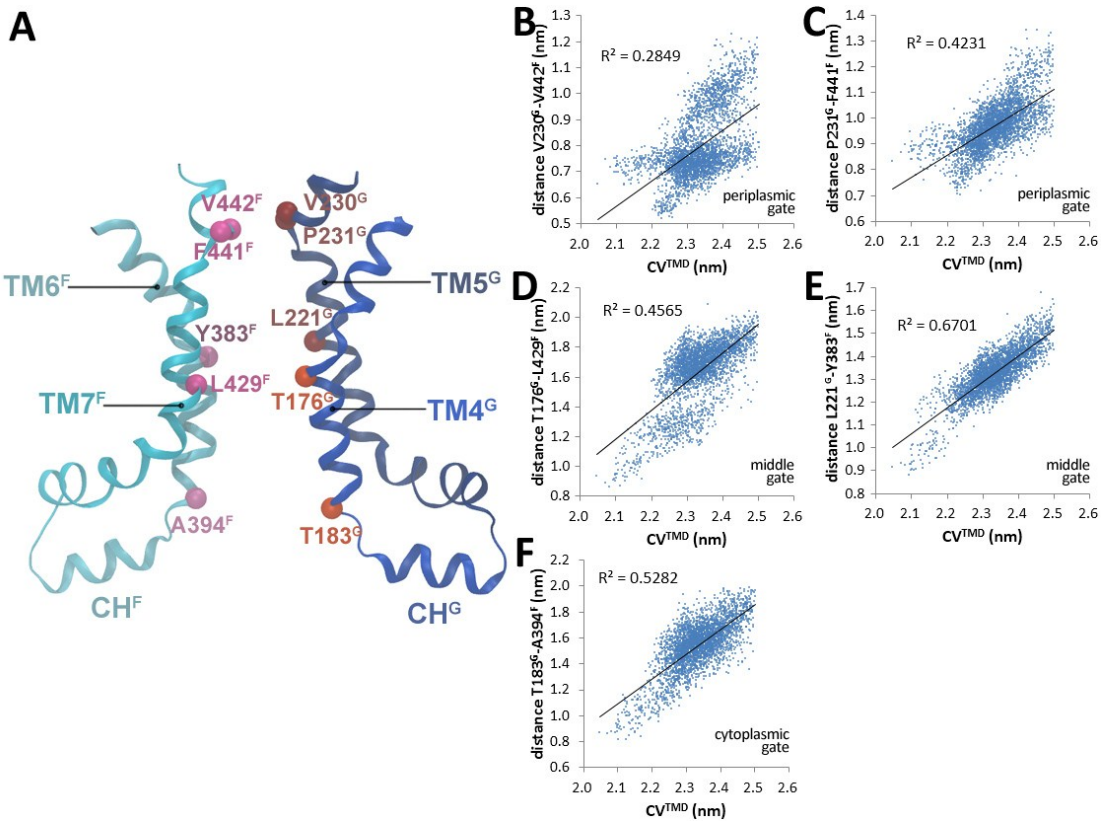

Figure S1. (A) The translocation pathway at the MalF-MalG interface. The residues forming the periplasmic, middle and cytoplasmic gates along the pathway are represented by their C_α atoms as spheres. The correlation of CV^{TMD} with the inter-residue distance $V230^{G}$-$V442^{F}$ (B) and $P231^{G}$-$F441^{F}$ (C) lying at the periplasmic side of TMDs, with the inter-residue distance $T176^{G}$-$L429^{F}$ (D) and $L221^{G}$-$Y383^{F}$ (E) in the middle of the TMHs, and with the inter-residue distance $T183^{G}$-$A394^{F}$ (F) at the cytoplasmic side. Metadynamics simulation trajectory of the **apo** system was projected onto the figures and the correlation coefficients were calculated supposing that all the snapshots share the same population.

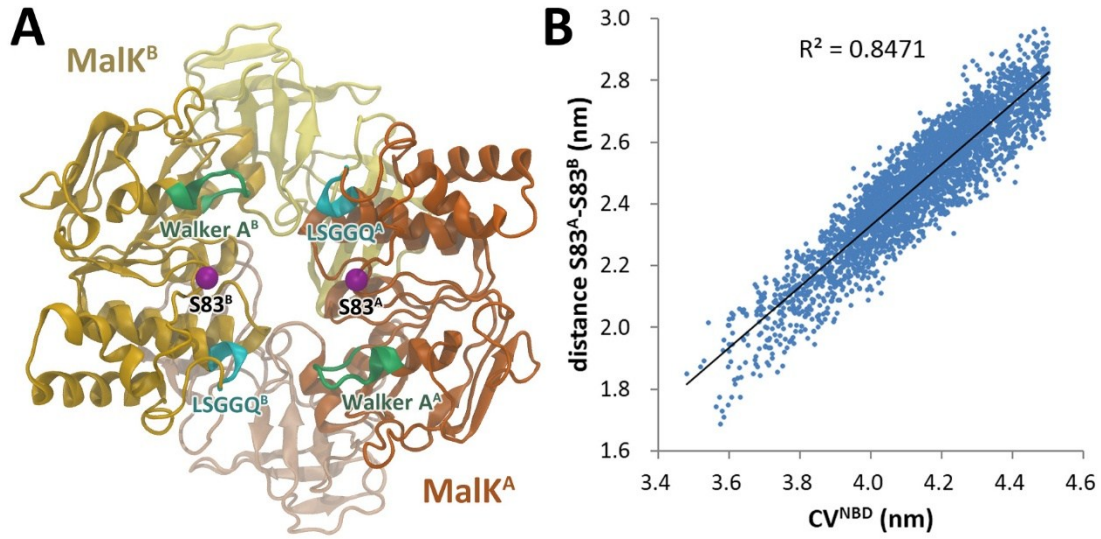

Figure S2. (A) NBD dimer interface viewed from the periplasm. The residues are represented by their C_α atoms as spheres. (B) Correlation between CV^{NBD} and the inter-residue distance $S83^A$-$S83^B$ in the metadynamics trajectory of the **apo** system. The correlation coefficient was calculated supposing that all the snapshots share the same population.

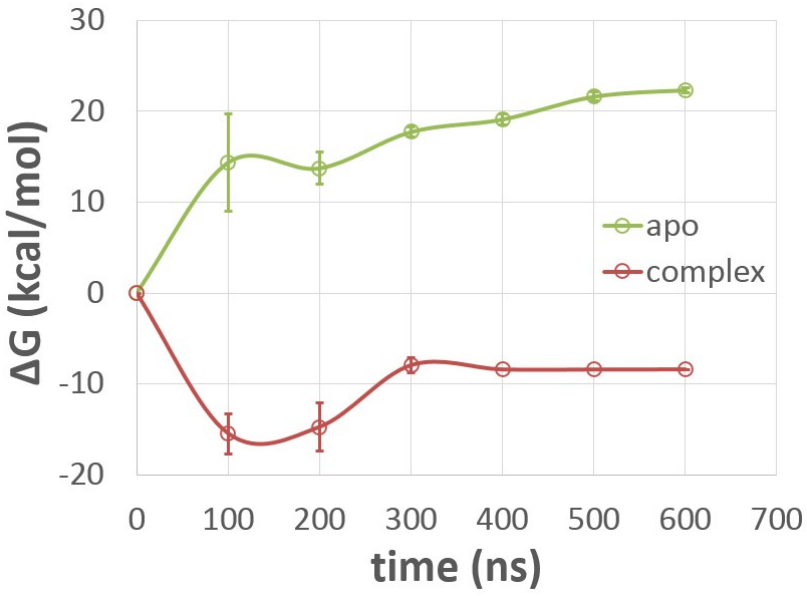

Figure S3. Convergence check of the metadynamics simulations of the **apo** and **complex** systems. The free energy differences between the pre-T and resting states on the 2-D space spanned by CV^{NBD} and CV^{TMD} are plotted against simulation time. For each point except time 0, the differences are averaged over the data within ±50 ns and the standard deviation for each average value is given as error bar.

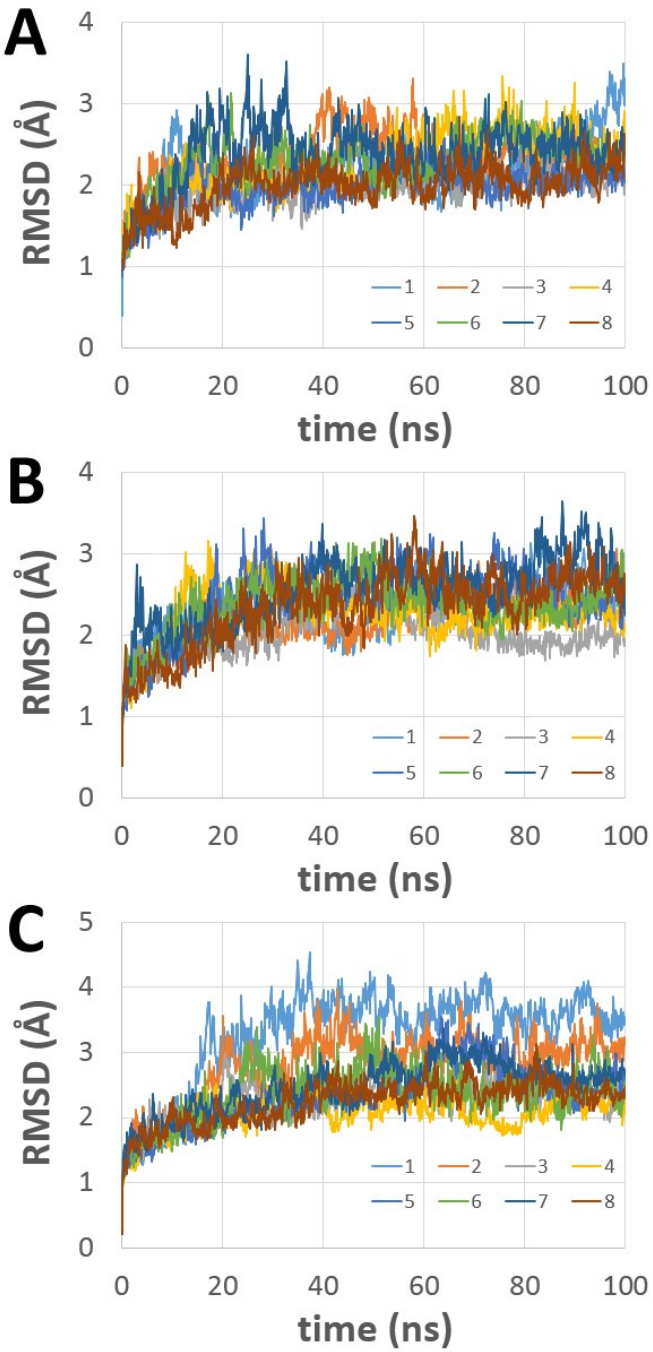

Figure S4. The variations of C_α root-mean-square deviations (RMSDs) along the eight 100-ns trajectories of the **complex** (A), **apo** (B), and **MalF500** (C) systems. C_α RMSD is defined relative to the initial structure.

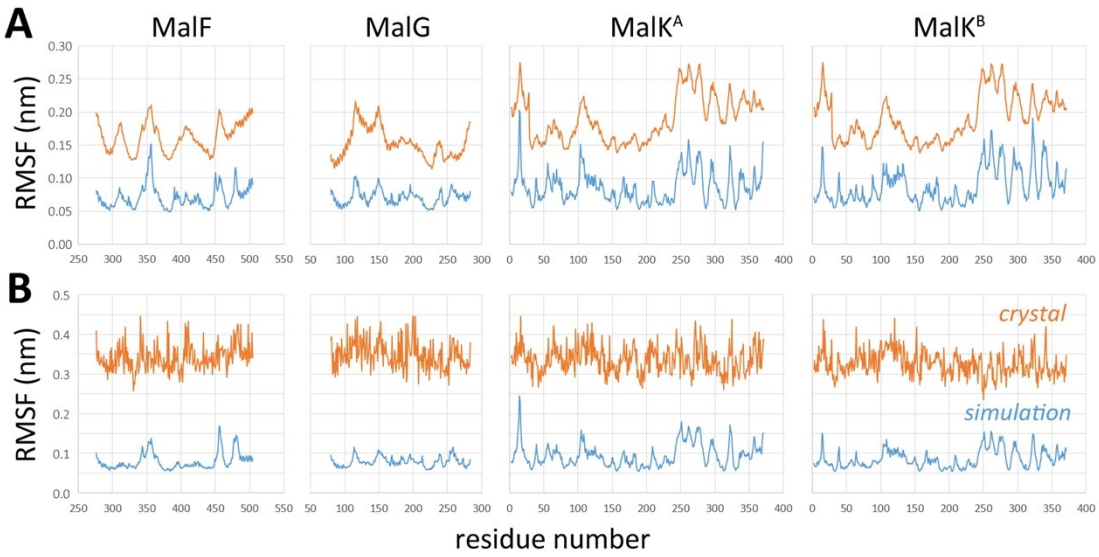

Figure S5. Comparison of the Cα RMSFs calculated from the unbiased MD simulations of **complex** (A) and **apo** (B) systems with those derived from the B-factors of the crystal structures. The RMSF values were calculated using the last 5 ns of each trajectory and were then averaged over the trajectories. Only the residues on MalFG cores or on MalKs were considered. For ease of comparison, the crystallographic B-factors were transformed into RMSFs according to the equation $RMSF = [3 \bullet \text{B-factor} / (8\pi^2)]^{1/2}$.

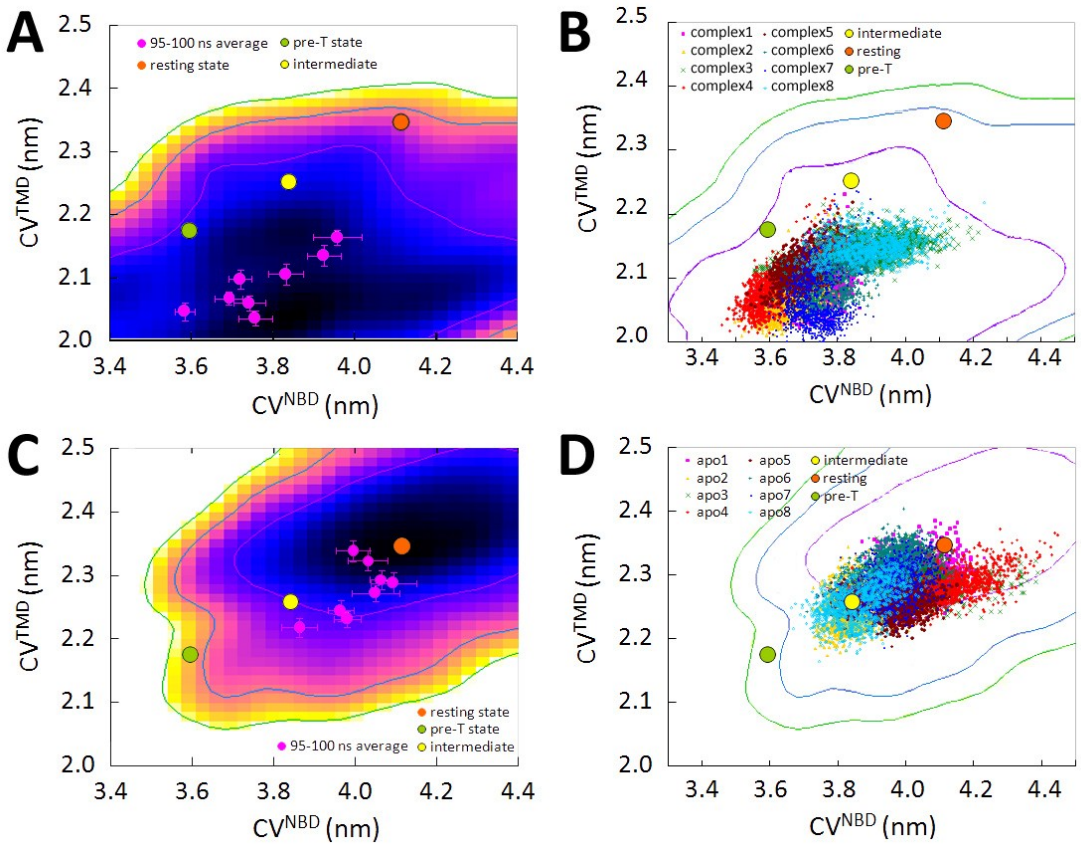

Figure S6. (A) Final structures of eight 100-ns **complex** trajectories initiated from an intermediate structure (yellow circle) projected on the 2-D space spanned by CV^{NBD} and CV^{TMD}. The final structures are averaged over the last 5 ns and the standard deviations of the CVs are denoted by error bars. The projections of the resting and pre-T states on the 2-D space are denoted by orange and green circles, respectively. (B) Snapshots of the 100-ns **complex** trajectories projected on the 2-D space. (C) Final structures of eight 100-ns **apo** trajectories projected on the 2-D space. (D) Snapshots of the 100-ns **apo** trajectories projected on the 2-D space. The 2-D energy landscape and/or the contour lines of the landscape denoting 10, 20, 30 kcal/mol obtained from metadynamics simulations are also depicted.